

Ground-state phase diagram, symmetries, excitation spectra and finite-frequency scaling of the two-mode quantum Rabi model

Yue Chen(陈越), Maoxin Liu(刘卯鑫), and Xiaosong Chen(陈晓松)
Citation: Chin. Phys. B, 2023, 32 (**10**): 104213. DOI: 10.1088/1674-1056/acea66
Journal homepage: http://cpb.iphy.ac.cn; http://iopscience.iop.org/cpb

What follows is a list of articles you may be interested in

Tunable magnomechanically induced transparency and fast-slow light in a hybrid cavity magnomechanical system

Qinghong Liao(廖庆洪), Kun Peng(彭坤), and Haiyan Qiu(邱海燕)
Chin. Phys. B, 2023, 32 (**5**): 054205. DOI: 10.1088/1674-1056/acaf2b

Nonreciprocal two-photon transmission and statistics in a chiral waveguide QED system

Lei Wang(王磊), Zhen Yi(伊珍), Li-Hui Sun(孙利辉), and Wen-Ju Gu(谷文举)
Chin. Phys. B, 2022, 31 (**5**): 054206. DOI: 10.1088/1674-1056/ac3ecc

Topological phases and type-II edge state in two-leg-coupled Su-Schrieffer-Heeger chains

Tianqi Luo(罗天琦), Xin Guan(关欣), Jingtao Fan(樊景涛), Gang Chen(陈刚), and Suo-Tang Jia(贾锁堂)
Chin. Phys. B, 2022, 31 (**1**): 014208. DOI: 10.1088/1674-1056/ac3650

Tunable optomechanically induced transparency and fast-slow light in a loop-coupled optomechanical system

Qinghong Liao(廖庆洪), Xiaoqian Wang(王晓倩), Gaoqian He(何高倩), and Liangtao Zhou(周良涛)
Chin. Phys. B, 2021, 30 (**9**): 094205. DOI: 10.1088/1674-1056/ac0cda

Controllable four-wave mixing response in a dual-cavity hybrid optomechanical system

Lei Shang(尚蕾), Bin Chen(陈彬), Li-Li Xing(邢丽丽), Jian-Bin Chen(陈建宾), Hai-Bin Xue(薛海斌), and Kang-Xian Guo(郭康贤)
Chin. Phys. B, 2021, 30 (**5**): 054209. DOI: 10.1088/1674-1056/abd695

Ground-state phase diagram, symmetries, excitation spectra and finite-frequency scaling of the two-mode quantum Rabi model

Yue Chen(陈越)[1,2], Maoxin Liu(刘卯鑫)[3], and Xiaosong Chen(陈晓松)[3,†]

[1] *CAS Key Laboratory of Theoretical Physics, Institute of Theoretical Physics, Chinese Academy of Sciences, Beijing* 100190, *China*
[2] *School of Physical Sciences, University of Chinese Academy of Sciences, Beijing* 100049, *China*
[3] *School of Systems Science, Beijing Normal University, Beijing* 100875, *China*

(Received 6 May 2023; revised manuscript received 22 June 2023; accepted manuscript online 26 July 2023)

We investigate the two-mode quantum Rabi model (QRM) describing the interaction between a two-level atom and a two-mode cavity field. The quantum phase transitions are found when the ratio η of transition frequency of atom to frequency of cavity field approaches infinity. We apply the Schrieffer–Wolff (SW) transformation to derive the low-energy effective Hamiltonian of the two-mode QRM, thus yielding the critical point and rich phase diagram of quantum phase transitions. The phase diagram consists of four regions: a normal phase, an electric superradiant phase, a magnetic superradiant phase and an electromagnetic superradiant phase. The quantum phase transition between the normal phase and the electric (magnetic) superradiant phase is of second order and associates with the breaking of the discrete Z_2 symmetry. On the other hand, the phase transition between the electric superradiant phase and the magnetic superradiant phase is of first order and relates to the breaking of the continuous $U(1)$ symmetry. Several important physical quantities, for example the excitation energy and average photon number in the four phases, are derived. We find that the excitation spectra exhibit the Nambu–Goldstone mode. We calculate analytically the higher-order correction and finite-frequency exponents of relevant quantities. To confirm the validity of the low-energy effective Hamiltonians analytically derived by us, the finite-frequency scaling relation of the averaged photon numbers is calculated by numerically diagonalizing the two-mode quantum Rabi Hamiltonian.

Keywords: two-mode quantum Rabi model, superradiant phase transition, Nambu–Goldstone mode, finite-frequency scaling, Schrieffer–Wolff (SW) transformation

PACS: 42.50.Ct, 05.30.Rt, 64.60.an, 12.38.Bx **DOI:** 10.1088/1674-1056/acea66

1. Introduction

The quantum phase transition (QPT) is an important issue in the area of quantum optics and condensed-matter physics.[1–14] Traditional studies of the quantum phase transition mostly focus on the thermodynamic limit, which requires the number of microparticles to approach infinity. However, recent theoretical studies show that a second-order quantum phase transition can occur when the ratio of atom transition frequency to cavity frequency approaches infinity whereas the system contains only one atom, such as the quantum Rabi model (QRM).[15,16]

The QRM describes the interaction between a photon field and a two-level system,[17,18] which is one of the simplest models for studying the light–matter interaction and plays a significant role in quantum optics,[19] quantum information[20] and condensed-matter physics.[21] The single-mode QRM can be realized experimentally by a photonic analog simulator, based on light transport in femtosecond-laser-written waveguide superlattices, which provides an experimentally accessible test bed to explore the physics of light–matter interaction in the deep strong coupling regime.[22] Recently, a trapped-ion experiment using a $^{171}Yb^{+}$ ion in a Paul trap observed this quantum phase transition, which opens up a new window for controllable study of the quantum phase transition without requiring the thermodynamic limit.[23] Moreover, Chen *et al.* experimentally simulated the occurrence of an equilibrium superradiant phase transition beyond the no-go theorem by introducing the antisqueezing effect based on the platform of nuclear magnetic resonance.[24] With the rapid experimental progress in accessing the strong,[25,26] the ultrastrong,[27–29] and the deep strong[30,31] coupling regimes, the QRM has received much attention.[32–54] Since the quantum phase transition and critical phenomena in the QRM are found, further study on the scaling behaviors of the Rabi and the Dicke models has revealed that these two models belong to the same universality class.[55] These progresses bring a new insight into the quantum phase transitions without the thermodynamic limit. However, how the number of cavity fields of QRM influences the quantum phase transition remains an open question. Moreover, the interaction between a two-mode cavity field and a three-level system leads to many important phenomena, such as electromagnetically induced transparency[56] and dark state,[57] which are profitable in the precise control of coherent population trapping and transfer.[58] The three-level system is also important in quantum information, referred to as qutrit. Compared with the two-level scheme, the quantum key distribution based on qutrits is more resistant to attack,[59,60] and the

†Corresponding author. E-mail: chenxs@bnu.edu.cn

© 2023 Chinese Physical Society and IOP Publishing Ltd

quantum computation using qutrits shows a faster speed and a lower error rate.[61,62] Hayn *et al.* studied quantum phase transitions by a generalized Holstein–Primakoff transformation and revealed that it exhibits two superradiant quantum phase transitions, which can be both of first and second orders.[63] Cordero *et al.* found that the polychromatic ground-state phase diagram can be divided into monochromatic regions by a variational analysis.[64] Zhang *et al.* reported an analytical calculation of the ground-state phase diagram, scaling function, and critical exponents for the two-mode three-level QRM.[8] However, the quantum phase transition in a two-mode photon field model with few degrees of freedom, i.e., the two-mode QRM, has not been extensively studied. In this work, we consider a two-level atom interacting with two different photonic field modes. Since the model symmetry shifts as the parameter of the model Hamiltonian changes, we expect there would arise rich critical phenomena. To identify the possible quantum phases and quantum phase transitions involved in a two-mode model is helpful in further understanding the light–matter interaction models and extending their applications.

The paper is organized as follows. In Section 2, the low-energy effective Hamiltonians for four different phases are derived when the ratio of the atom frequency to the photon frequency approaches infinity and the ground-state phase diagram is obtained. In Section 3, the symmetries of two-mode QRM are studied. In Section 4, the excitation spectra, critical photon number and fluctuations of field quadratures are analytically calculated. In Section 5, the finite-frequency exponents are analytically derived and the finite-frequency scaling relations of average photon numbers are verified numerically. Finally, a brief summary and conclusions are presented in Section 6.

2. The effective Hamiltonian and ground-state phase diagram

The two-mode quantum Rabi model (QRM) describes the interaction between two cavity fields and one two-level atom. Its Hamiltonian is

$$\begin{aligned} H \;=\; & \omega a^{\dagger}a+\omega b^{\dagger}b+\frac{\Omega}{2}\sigma_z+\lambda_1(a^{\dagger}+a)(\sigma_{+}+\sigma_{-}) \\ & +\lambda_2(b^{\dagger}-b)(\sigma_{+}-\sigma_{-}), \end{aligned} \tag{1}$$

where σ_z is the Pauli matrix for a two-level atom, σ_+ and σ_- are the raising and lowering operators of spin respectively, and a ($a^{\dagger}$) and b ($b^{\dagger}$) are the annihilation (creation) operators for two cavity fields respectively. The parameters ω, Ω, λ_1, and λ_2 are the cavity field frequency, transition frequency of the atom and the coupling strength parameters respectively. The coupling of the first cavity field a with spin represents the interaction of the electric field with atom, while that of the second cavity field b with spin represents the interaction of magnetic field with atom. Such a coupling mechanism has been investigated in the single-mode QRM and can be implemented in circuit quantum electrodynamics systems, where artificial Josephson atoms are coupled both capacitively and inductively to a superconducting resonator.[65] It has also been studied in the two-mode Dicke model[66] and experimentally realized with continuous translational symmetry breaking along one direction in a quantum gas.[67]

Here $|\downarrow\rangle$ and $|\uparrow\rangle$ are the low-energy and high-energy eigenstates of σ_z respectively. $|m_1\rangle$ and $|m_2\rangle$ (m_1, $m_2 \in N$) are the eigenstates of $a^{\dagger}a$ and $b^{\dagger}b$ respectively. The parity operator $\Pi = \mathrm{e}^{\mathrm{i}\pi[a^{\dagger}a+b^{\dagger}b+\frac{1}{2}(1+\sigma_z)]}$ measures the odd–even parity of total excitation number and commutes with H. Though there is an exact solution for the one-mode QRM,[39] a lack of a closed-form solution makes it not directly applicable to investigate the QPT, thus the approximately analytical and the numerical methods are applied to study the QPT. The same situation exists for the two-mode QRM. When the system approaches the classical regime, the mean-field approximation is effective, but when the system is completely quantum, it fails. To settle this problem, we apply Schrieffer–Wolff (SW) transformation to derive the low-energy effective Hamiltonian of the two-mode QRM.

Based on the SW transformation, in the limit $\eta = \Omega/\omega \to \infty$, we find a unitary transformation

$$U = \frac{1}{\Omega}[\lambda_1(a^{\dagger}+a)(\sigma_{+}-\sigma_{-})+\lambda_2(b^{\dagger}-b)(\sigma_{+}+\sigma_{-})], \tag{2}$$

which makes the transformed Hamiltonian $UHU^{\dagger}$ free of coupling terms between spin subspaces $\mathcal{H}_{\downarrow}$ and $\mathcal{H}_{\uparrow}$. Neglecting the high-order terms and under the condition $\eta \gg 1$, the effective Hamiltonian is

$$\begin{aligned} H_{\mathrm{eff}} \;\approx\; & \omega a^{\dagger}a+\omega b^{\dagger}b+\frac{\Omega}{2}\sigma_z \\ & -\frac{1}{\Omega}\left[\lambda_1^2(a^{\dagger}+a)^2-\lambda_2^2(b^{\dagger}-b)^2\right] \\ & +\frac{1}{\Omega^3}\left[\lambda_1^2(a^{\dagger}+a)^2-\lambda_2^2(b^{\dagger}-b)^2\right]^2. \end{aligned} \tag{3}$$

Considering the limit $\eta = \Omega/\omega \to \infty$, and projecting the Hamiltonian to the spin-down subspace, we can obtain the effective Hamiltonian of the normal phase (NP) as

$$H_{\mathrm{np}} = \omega a^{\dagger}a+\omega b^{\dagger}b-\frac{\Omega}{2}-\frac{\omega}{4}[g_1^2(a^{\dagger}+a)^2-g_2^2(b^{\dagger}-b)^2], \tag{4}$$

where $g_1 = 2\lambda_1/\sqrt{\omega\Omega}$ and $g_2 = 2\lambda_2/\sqrt{\omega\Omega}$. By applying unitary transformations with squeezing operators $\mathcal{S}_1(r_{1,\mathrm{np}}) = \exp[(r_{1,\mathrm{np}}/2)(a^{\dagger 2}-a^2)]$ and $\mathcal{S}_2(r_{2,\mathrm{np}}) = \exp[(r_{2,\mathrm{np}}/2)(b^{\dagger 2}-b^2)]$ to H_{np}, the diagonalized Hamiltonian can be obtained as

$$H'_{\mathrm{np}} = \varepsilon_{1,\mathrm{np}}a^{\dagger}a+\varepsilon_{2,\mathrm{np}}b^{\dagger}b+E_{\mathrm{G,np}}, \tag{5}$$

where

$$\varepsilon_{1,\mathrm{np}} = \omega\sqrt{1-g_1^2}, \quad \varepsilon_{2,\mathrm{np}} = \omega\sqrt{1-g_2^2}, \tag{6}$$

which are the excitation energy of two cavity fields, respectively, and

$$E_{\mathrm{G,np}}=\frac{1}{2}(\varepsilon_{1,\mathrm{np}}+\varepsilon_{2,\mathrm{np}})-\omega-\frac{\Omega}{2} \tag{7}$$

is the ground state energy. The energy eigenvalues and eigenstates in the NP are respectively

$$E_{\mathrm{np}}^{m_1m_2}(g_1,g_2)=\varepsilon_{1,\mathrm{np}}m_1+\varepsilon_{2,\mathrm{np}}m_2+E_{\mathrm{G,np}}, \tag{8}$$

$$\left|\phi_{\mathrm{np}}^{m_1m_2}(g_1,g_2)\right\rangle=\mathcal{S}_2^{\dagger}[r_{2,\mathrm{np}}(g_2)]\mathcal{S}_1^{\dagger}[r_{1,\mathrm{np}}(g_1)]\left|m_1,m_2,\downarrow\right\rangle, \tag{9}$$

with $r_{1,\mathrm{np}}=\ln(1-g_1^2)/4$, $r_{2,\mathrm{np}}=-\ln(1-g_2^2)/4$. Since $E_{\mathrm{G,np}}$ must be real, for the NP we have $g_1\leqslant 1$, $g_2\leqslant 1$. Hence the critical points of the QPT are $g_1=g_2=g_{\mathrm{c}}=1$.

For $g_1>1$ or $g_2>1$, the Eq. (4) fails, indicating the number of photons occupied in the cavity fields becomes proportional to η so that the higher-order terms cannot be neglected, i.e., the ground state comes into the superradiant phase. It also suggests the low-energy subspace changes. In order to obtain the new low-energy effective Hamiltonian, we transform the original two-mode quantum Rabi Hamiltonian by displaying two field modes a and b with displacement operators $\mathcal{D}_1(\alpha)=\mathrm{e}^{\alpha(a^{\dagger}-a)}$ and $\mathcal{D}_2(\beta)=\mathrm{e}^{\mathrm{i}\beta(b^{\dagger}+b)}$, where α and β are real,

$$\begin{aligned}\tilde{H}(\alpha,\beta) &= \mathcal{D}_2(\beta)\mathcal{D}_1(\alpha)H\mathcal{D}_1^{\dagger}(\alpha)\mathcal{D}_2^{\dagger}(\beta)\\ &= \omega a^{\dagger}a+\omega b^{\dagger}b+\lambda_1(a^{\dagger}+a)(\sigma_{+}+\sigma_{-})\\ &\quad+\lambda_2(b^{\dagger}-b)(\sigma_{+}-\sigma_{-})\\ &\quad-\omega\alpha(a^{\dagger}+a)-\mathrm{i}\omega\beta(b^{\dagger}-b)+\omega(\alpha^2+\beta^2)\\ &\quad+\frac{\Omega}{2}\sigma_z-2\lambda_1\alpha\sigma_x-2\lambda_2\beta\sigma_y.\end{aligned} \tag{10}$$

The eigenstates of atomic part of Hamiltonian, i.e., $(\Omega/2)\sigma_z-2\lambda_1\alpha\sigma_x-2\lambda_2\beta\sigma_y$, are

$$\begin{cases}\left|\tilde{\uparrow}\right\rangle=\frac{1}{\sqrt{2\tilde{\Omega}(\tilde{\Omega}-\Omega)}}\begin{bmatrix}4(\lambda_1\alpha-\mathrm{i}\lambda_2\beta)\\ \Omega-\tilde{\Omega}\end{bmatrix},\\ \left|\tilde{\downarrow}\right\rangle=\frac{1}{\sqrt{2\tilde{\Omega}(\tilde{\Omega}+\Omega)}}\begin{bmatrix}4(\lambda_1\alpha-\mathrm{i}\lambda_2\beta)\\ \Omega+\tilde{\Omega}\end{bmatrix},\end{cases} \tag{11}$$

where the new transition frequency

$$\tilde{\Omega}=\sqrt{\Omega^2+16(\lambda_1^2\alpha^2+\lambda_2^2\beta^2)}.$$

In the new representation, after expressing σ_x,σ_y, and σ_z in the terms of $\tilde{\sigma}_x,\tilde{\sigma}_y$, and $\tilde{\sigma}_z$ and substituting them into Eq. (10), the displaced Hamiltonian can be expressed as

$$\begin{aligned}\tilde{H} &= \omega a^{\dagger}a+\omega b^{\dagger}b+\frac{\tilde{\Omega}}{2}\tilde{\sigma}_z+\omega(\alpha^2+\beta^2)\\ &\quad+\frac{\Omega\lambda_1^2\alpha}{\tilde{\Omega}\sqrt{\lambda_1^2\alpha^2+\lambda_2^2\beta^2}}(a^{\dagger}+a)\tilde{\sigma}_x\\ &\quad+\frac{\mathrm{i}\lambda_1\lambda_2\alpha}{\sqrt{\lambda_1^2\alpha^2+\lambda_2^2\beta^2}}(b^{\dagger}-b)\tilde{\sigma}_y\\ &\quad-\frac{\lambda_1\lambda_2\beta}{\sqrt{\lambda_1^2\alpha^2+\lambda_2^2\beta^2}}(a^{\dagger}+a)\tilde{\sigma}_y\\ &\quad+\frac{\mathrm{i}\Omega\lambda_2^2\beta}{\tilde{\Omega}\sqrt{\lambda_1^2\alpha^2+\lambda_2^2\beta^2}}(b^{\dagger}-b)\tilde{\sigma}_x\\ &\quad-\alpha(\omega+\frac{4\lambda_1^2}{\tilde{\Omega}}\tilde{\sigma}_z)(a^{\dagger}+a)\\ &\quad-\mathrm{i}\beta(\omega+\frac{4\lambda_2^2}{\tilde{\Omega}}\tilde{\sigma}_z)(b^{\dagger}-b).\end{aligned} \tag{12}$$

The requirement that the block-diagonal perturbation terms vanish in the last line gives

$$\begin{cases}\alpha(\omega-\frac{4\lambda_1^2}{\tilde{\Omega}})=0,\\ \beta(\omega-\frac{4\lambda_2^2}{\tilde{\Omega}})=0.\end{cases} \tag{13}$$

There are three sets of solutions of the above equations, and the ground-state energy of Hamiltonians corresponding to the above solutions is discussed as follows.

(i) The first mode a is displaced with the second mode b unchanged. We have

$$\alpha=\pm\alpha_{g_1}=\pm\frac{1}{2}\sqrt{\eta(g_1^2-g_1^{-2})},\ \ \beta=0,\ \ \tilde{\Omega}=g_1^2\Omega. \tag{14}$$

Substituting Eq. (14) into Eq. (12), and applying SW transformation again, we can obtain the low-energy effective Hamiltonian as

$$\begin{aligned}\tilde{H}_{\mathrm{esp}} &= \omega a^{\dagger}a+\omega b^{\dagger}b-\frac{\Omega}{4}(g_1^2+g_1^{-2})\\ &\quad-\frac{1}{\tilde{\Omega}}[\tilde{\lambda}_1^2(a^{\dagger}+a)^2-\lambda_2^2(b^{\dagger}-b)^2],\end{aligned} \tag{15}$$

where the subscript esp denotes electric superradiant phase (ESP) and the rescaled coupling parameter $\tilde{\lambda}_1=\sqrt{\omega\Omega}/(2g_1)$. To diagonalize the above Hamiltonian, we take two successive unitary transformations to the Hamiltonian with the squeezing operators $\mathcal{S}_1(r_{1,\mathrm{esp}})=\exp[(r_{1,\mathrm{esp}}/2)(a^{\dagger 2}-a^2)]$ and $\mathcal{S}_2(r_{2,\mathrm{esp}})=\exp[(r_{2,\mathrm{esp}}/2)(b^{\dagger 2}-b^2)]$. Making the off-diagonal terms in the new Hamiltonian equal to zero, the parameters in the squeezing operators are solved as $r_{1,\mathrm{esp}}=\ln(1-g_1^{-4})/4$, $r_{2,\mathrm{esp}}=-\ln\left(1-g_2^2/g_1^2\right)/4$. The transformed Hamiltonian and the ground-state energy are respectively

$$\tilde{H}'_{\mathrm{esp}}=\varepsilon_{1,\mathrm{esp}}a^{\dagger}a+\varepsilon_{2,\mathrm{esp}}b^{\dagger}b+E_{\mathrm{G,esp}}, \tag{16}$$

$$E_{\mathrm{G,esp}}=\frac{1}{2}(\varepsilon_{1,\mathrm{esp}}+\varepsilon_{2,\mathrm{esp}})-\omega-\frac{\Omega}{4}(g_1^2+g_1^{-2}), \tag{17}$$

where the excitation energy of two cavity fields are respectively

$$\varepsilon_{1,\mathrm{esp}}=\omega\sqrt{1-g_1^{-4}},\ \ \varepsilon_{2,\mathrm{esp}}=\omega\sqrt{1-\frac{g_2^2}{g_1^2}}. \tag{18}$$

The energy eigenvalues and eigenstates in the ESP are respectively

$$E_{\rm esp}^{m_1m_2}(g_1,g_2)=\varepsilon_{1,\rm esp}m_1+\varepsilon_{2,\rm esp}m_2+E_{\rm G,esp}, \tag{19}$$

$$\left|\phi_{\rm esp}^{m_1m_2}(g_1,g_2)\right\rangle_{\pm}=\mathcal{D}_1^{\dagger}(\pm\alpha_{g_1})\mathcal{S}_2^{\dagger}[r_{2,\rm esp}(g_1,g_2)] \times\mathcal{S}_1^{\dagger}[r_{1,\rm esp}(g_1)]\left|m_1,m_2,\downarrow^{\pm}\right\rangle, \tag{20}$$

where

$$\left|\downarrow^{\pm}\right\rangle=\pm\sqrt{\frac{1-g_1^{-2}}{2}}\left|\uparrow\right\rangle+\sqrt{\frac{1+g_1^{-2}}{2}}\left|\downarrow\right\rangle. \tag{21}$$

The eigenstates are degenerate and have a spontaneous broken parity symmetry as we can see from nonzero coherence of the field $\langle a\rangle=\pm\alpha_g$ and $\langle b\rangle=\pm\beta_g$. To ensure the ground state energy is real, g_1 and g_2 have to satisfy $g_1\geqslant 1$, $g_1\geqslant g_2$.

(ii) The second mode b is displaced with the first mode a unchanged. We have

$$\alpha=0,\ \ \beta=\pm\beta_{g_2}=\pm\frac{1}{2}\sqrt{\eta(g_2^2-g_2^{-2})},\ \ \tilde{\Omega}=g_2^2\Omega. \tag{22}$$

Similar as before, we can obtain the low-energy effective Hamiltonian as

$$\tilde{H}_{\rm msp}=\omega a^{\dagger}a+\omega b^{\dagger}b-\frac{\Omega}{4}(g_2^2+g_2^{-2}) -\frac{1}{\tilde{\Omega}}[\lambda_1^2(a^{\dagger}+a)^2-\tilde{\lambda}_2^2(b^{\dagger}-b)^2], \tag{23}$$

where the subscript msp denotes magnetic superradiant phase (MSP) and the rescaled coupling parameter $\tilde{\lambda}_2=\sqrt{\omega\Omega}/2g_2$. We take two successive unitary transformations to the Hamiltonian with the squeezing operators $\mathcal{S}_1(r_{1,\rm msp})=\exp\left[(r_{1,\rm msp}/2)(a^{\dagger 2}-a^2)\right]$ and $\mathcal{S}_2(r_{2,\rm msp})=\exp\left[(r_{2,\rm msp}/2)(b^{\dagger 2}-b^2)\right]$ with the parameters $r_{1,\rm msp}=\ln\left(1-g_1^2/g_2^2\right)/4$, $r_{2,\rm msp}=-\ln(1-g_2^{-4})/4$. The transformed Hamiltonian and the ground states energy are respectively

$$\tilde{H}'_{\rm msp}=\varepsilon_{1,\rm msp}a^{\dagger}a+\varepsilon_{2,\rm msp}b^{\dagger}b+E_{\rm G,msp}, \tag{24}$$

$$E_{\rm G,msp}=\frac{1}{2}(\varepsilon_{1,\rm msp}+\varepsilon_{2,\rm msp})-\omega-\frac{\Omega}{4}(g_2^2+g_2^{-2}), \tag{25}$$

where the excitation energy of two cavity fields are respectively

$$\varepsilon_{1,\rm msp}=\omega\sqrt{1-\frac{g_1^2}{g_2^2}},\ \ \varepsilon_{2,\rm msp}=\omega\sqrt{1-g_2^{-4}}. \tag{26}$$

The energy eigenvalues and eigenstates in the MSP are respectively

$$E_{\rm msp}^{m_1m_2}(g_1,g_2)=\varepsilon_{1,\rm msp}m_1+\varepsilon_{2,\rm msp}m_2+E_{\rm G,msp}, \tag{27}$$

$$\left|\phi_{\rm msp}^{m_1m_2}(g_1,g_2)\right\rangle_{\pm}=\mathcal{D}_2^{\dagger}(\pm\beta_{g_2})\mathcal{S}_2^{\dagger}[r_{2,\rm msp}(g_2)] \times\mathcal{S}_1^{\dagger}[r_{1,\rm msp}(g_1,g_2)]\left|m_1,m_2,\downarrow^{\pm}\right\rangle, \tag{28}$$

where

$$\left|\downarrow^{\pm}\right\rangle=\pm{\rm i}\sqrt{\frac{1-g_2^{-2}}{2}}\left|\uparrow\right\rangle+\sqrt{\frac{1+g_2^{-2}}{2}}\left|\downarrow\right\rangle. \tag{29}$$

To ensure the ground state energy is real, g_1 and g_2 have to satisfy $g_2\geqslant 1$, $g_2\geqslant g_1$.

(iii) Both the mode a and b are displaced, we have

$$\begin{cases}\alpha\neq 0,\quad \beta\neq 0,\\ g=g_1=g_2,\\ \alpha^2+\beta^2=(\eta/4)(g^2-g^{-2}),\\ \tilde{\Omega}=g^2\Omega.\end{cases} \tag{30}$$

In this set of solution, the values of α and β are not unique. We suppose $\beta=\mu\alpha,\mu\in(-\infty,\infty)$ and $\mu\neq 0$, thus from the above equations we obtain

$$\alpha=\pm\alpha_g=\pm\frac{1}{2\sqrt{1+\mu^2}}\sqrt{\eta(g^2-g^{-2})}, \tag{31}$$

$$\beta=\pm\beta_g=\pm\frac{\mu}{2\sqrt{1+\mu^2}}\sqrt{\eta(g^2-g^{-2})}. \tag{32}$$

Substituting Eqs. (31) and (32) into Eq. (12), by the approach of SW transformation, the low-energy effective Hamiltonian of electromagnetic superradiant phase (EMSP) is

$$\tilde{H}_{\rm emsp}=\omega a^{\dagger}a+\omega b^{\dagger}b-\frac{\Omega}{4}(g^2+g^{-2}) -\frac{1}{\tilde{\Omega}}[\lambda_1'^2(a^{\dagger}+a)^2-\lambda_2'^2(b^{\dagger}-b)^2], \tag{33}$$

where

$$\lambda_1'=\lambda\sqrt{(\mu^2+g^{-4})/(1+\mu^2)},$$
$$\lambda_2'=\lambda\sqrt{(1+\mu^2g^{-4})/(1+\mu^2)}.$$

We take two successive unitary transformations to the Hamiltonian with the squeezing operators $\mathcal{S}_1(r_{1,\rm emsp})=\exp[(r_{1,\rm emsp}/2)(a^{\dagger 2}-a^2)]$ and $\mathcal{S}_2(r_{2,\rm emsp})=\exp[(r_{2,\rm emsp}/2)(b^{\dagger 2}-b^2)]$ with the parameters $r_{1,\rm emsp}=(1/4)\ln((1-g^{-4})/(1+\mu^2))$, $r_{2,\rm emsp}=-(1/4)\ln(\mu^2(1-g^{-4})/(1+\mu^2))$. The transformed Hamiltonian and the ground states energy are respectively

$$\tilde{H}'_{\rm emsp}=\varepsilon_{1,\rm emsp}a^{\dagger}a+\varepsilon_{2,\rm emsp}b^{\dagger}b+E_{\rm G,emsp}, \tag{34}$$

$$E_{\rm G,emsp}=\frac{1}{2}(\varepsilon_{1,\rm emsp}+\varepsilon_{2,\rm emsp})-\omega-\frac{\Omega}{4}(g^2+g^{-2}), \tag{35}$$

where the single-photon energy of two cavity fields are respectively

$$\varepsilon_{1,\rm emsp}=\omega\sqrt{\frac{1-g^{-4}}{1+\mu^2}},\ \ \varepsilon_{2,\rm emsp}=\omega\sqrt{\frac{\mu^2(1-g^{-4})}{1+\mu^2}}. \tag{36}$$

The energy eigenvalues and eigenstates in the EMSP are respectively

$$E_{\rm emsp}^{m_1m_2}(g)=\varepsilon_{1,\rm emsp}m_1+\varepsilon_{2,\rm emsp}m_2+E_{\rm G,emsp}, \tag{37}$$

$$\left|\phi_{\rm emsp}^{m_1m_2}(g)\right\rangle_{\pm} = \mathcal{D}_2^{\dagger}(\pm\beta_g)\mathcal{D}_1^{\dagger}(\pm\alpha_g)\mathcal{S}_2^{\dagger}[r_{2,\rm emsp}(g)] \times \mathcal{S}_1^{\dagger}[r_{1,\rm emsp}(g)]\left|m_1,m_2,\downarrow^{\pm}\right\rangle, \quad (38)$$

where

$$\left|\downarrow^{\pm}\right\rangle = \pm\frac{1-\mathrm{i}\mu}{\sqrt{1+\mu^2}}\sqrt{\frac{1-g^{-2}}{2}}\left|\uparrow\right\rangle + \sqrt{\frac{1+g^{-2}}{2}}\left|\downarrow\right\rangle. \quad (39)$$

To ensure the ground state energy is real, g_1 and g_2 have to satisfy $g_1 = g_2 = g \geqslant 1$.

In the above three cases, if not equal to zero, there are two values for $\alpha = \pm\alpha_g$ or $\beta = \pm\beta_g$, leading to an identical spectrum, which is correlated with the parity symmetry of the system. The high-order corrections in Eqs. (4), (15), (23), and (33) vanish in the $\eta \to \infty$ limit, therefore the $H_{\rm np}, H_{\rm esp}, H_{\rm msp}$ and $H_{\rm emsp}$ are exact low-energy effective Hamiltonian for the NP, ESP, MSP and EMSP respectively. The Eqs. (7), (17), (25), and (35) give the ground state energy of four phases respectively. Take the limit $\eta \to \infty$, the rescaled ground state energy of four phases are respectively

$$e_{\rm G,np} = \frac{1}{\eta}E_{\rm G,np} = -\frac{\omega}{2}, \quad (40)$$

$$e_{\rm G,esp} = \frac{1}{\eta}E_{\rm G,esp} = -\frac{\omega}{4}(g_1^2 + g_1^{-2}), \quad (41)$$

$$e_{\rm G,msp} = \frac{1}{\eta}E_{\rm G,msp} = -\frac{\omega}{4}(g_2^2 + g_2^{-2}), \quad (42)$$

$$e_{\rm G,emsp} = \frac{1}{\eta}E_{\rm G,emsp} = -\frac{\omega}{4}(g^2 + g^{-2}). \quad (43)$$

The above exact solutions show that $g_1 = 1, g_2 = 1$ is the quadruple point. The phase diagram is displayed in the Fig. 1.

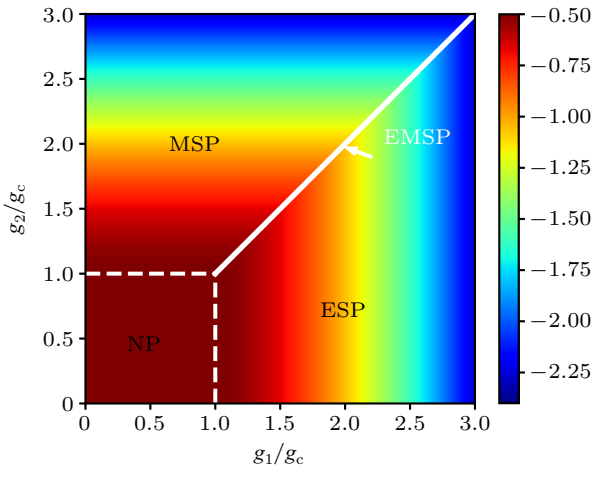


Fig. 1. The ground-state phase diagram as a function of g_1/g_c and g_2/g_c. The regime $g_1/g_c < 1$ and $g_2/g_c < 1$ denotes the normal phase (NP). The regime $g_1/g_c \geqslant 1$ and $g_1/g_c > g_2/g_c$ denotes the electric superradiant phase (ESP). The regime $g_1/g_c \geqslant 1$ and $g_2/g_c > g_1/g_c$ denotes the magnetic superradiant phase (MSP). The white solid line denotes the electromagnetic superradiant phase (EMSP) with regime $g_1/g_c = g_2/g_c \geqslant 1$.

For the phase transition from the NP to the ESP,

$$e_{\rm G,np}(g_1 = 1) = e_{\rm G,esp}(g_1 = 1), \quad (44)$$

$$\left.\frac{\mathrm{d}e_{\rm G,np}}{\mathrm{d}g_1}\right|_{g_1=1} = \left.\frac{\mathrm{d}e_{\rm G,esp}}{\mathrm{d}g_1}\right|_{g_1=1}, \quad (45)$$

$$\left.\frac{\mathrm{d}^2e_{\rm G,np}}{\mathrm{d}g_1^2}\right|_{g_1=1} \neq \left.\frac{\mathrm{d}^2e_{\rm G,esp}}{\mathrm{d}g_1^2}\right|_{g_1=1}. \quad (46)$$

Therefore, this phase transition is of second order. Similarly, it is not hard to confirm that the phase transition from the NP to the MSP is also of second order. When considering the phase transition from the ESP to the MSP, we take the derivatives of $e_{\rm G,esp}$ and $e_{\rm G,msp}$ along the unit vector $\boldsymbol{n} = -(1/\sqrt{2})(\boldsymbol{x} - \boldsymbol{y})$ where $\boldsymbol{x}$ and $\boldsymbol{y}$ are unit vectors along the horizontal and vertical axes respectively. There are

$$e_{\rm G,esp}(g_1 = g_2) = e_{\rm G,msp}(g_1 = g_2), \quad (47)$$

$$\frac{\mathrm{d}e_{\rm G,esp}}{\mathrm{d}\boldsymbol{n}}|_{g_1=g_2} \neq \frac{\mathrm{d}e_{\rm G,msp}}{\mathrm{d}\boldsymbol{n}}|_{g_1=g_2}. \quad (48)$$

Therefore the phase transition from the ESP to the MSP is of first order. In Fig. 2, we plot the rescaled ground-state energy, its first-order and second-order derivatives from the NP to the ESP. It is obvious that $e_{\rm G}$ and $\mathrm{d}e_{\rm G}/\mathrm{d}g_1$ are continuous at $g_1 = 1.0$, while $\mathrm{d}^2e_{\rm G}/\mathrm{d}g_1^2$ is not. Since the symmetry of the phase diagram, for the phase transition from NP to MSP, the ground-state energy, its first-order and second-order derivatives are similar with that of the phase transition from NP to ESP. See Appendix A for a detailed derivation of the effective Hamiltonians and their analytical diagonalization.

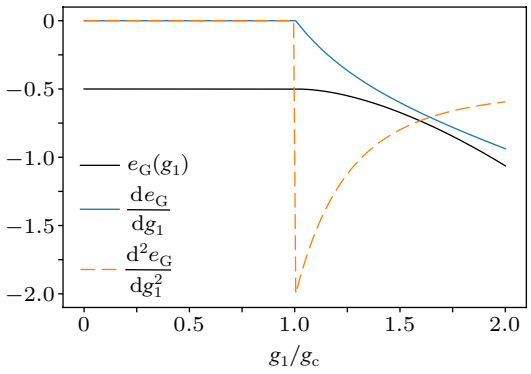


Fig. 2. The ground-state energy $e_{\rm G}$, its first-order derivative $\mathrm{d}e_{\rm G}/\mathrm{d}g_1$ and second-order derivative $\mathrm{d}^2e_{\rm G}/\mathrm{d}g_1^2$ from the NP to the ESP. For simplicity, we take $\omega = 1.0$. We can see that $e_{\rm G}$ and $\mathrm{d}e_{\rm G}/\mathrm{d}g_1$ are continuous at $g_1 = 1.0$, while $\mathrm{d}^2e_{\rm G}/\mathrm{d}g_1^2$ is not. Thus the phase transition from NP to ESP is of second-order.

3. Symmetries

To understand the phase transition, it is necessary to discuss the breaking of symmetries. Firstly, the Hamiltonian (1) has a discrete Z_2 symmetry. Take a transformation: $x \to -x$, $y \to -y$, we have

$$H[a^{\dagger}+a, b^{\dagger}-b, \sigma_+ + \sigma_-, \sigma_+ - \sigma_-] = H[-(a^{\dagger}+a), -(b^{\dagger}-b), -(\sigma_+ + \sigma_-), -(\sigma_+ - \sigma_-)]. \quad (49)$$

It is known from Eqs. (20), (21), (28), and (29) that the ground states of ESP and MSP are doubly degenerate. Therefore, the

phase transition from the NP to the ESP (MSP) is associated with the breaking of the discrete Z_2 symmetry.

When $\lambda_1 = \lambda_2 = \lambda$, the Hamiltonian becomes

$$\begin{aligned} H_\lambda &= \omega a^\dagger a + \omega b^\dagger b + \frac{\Omega}{2}\sigma_z + \lambda(a^\dagger + a)(\sigma_+ + \sigma_-) \\ &\quad + \lambda(b^\dagger - b)(\sigma_+ - \sigma_-). \end{aligned} \tag{50}$$

For the above Hamiltonian, we find a conserved quantity

$$C = a^\dagger b + a b^\dagger - \frac{1}{2}\sigma_z, \tag{51}$$

which satisfies $[H, C] = 0$ and results in a continuous $U(1)$ symmetry. To prove it, we introduce a unitary operator $U_\theta = \mathrm{e}^{\mathrm{i}\theta(a^\dagger b + a b^\dagger - \frac{1}{2}\sigma_z)}$ to perform a unitary transformation to the Hamiltonian (50) so that

$$\begin{aligned} H_U &= U_\theta H U_\theta^\dagger \\ &= \omega a^\dagger a + \omega b^\dagger b + \frac{\Omega}{2}\sigma_z \\ &\quad + (\lambda_1 \cos^2\theta + \lambda_2 \sin^2\theta)(a^\dagger + a)(\sigma_+ + \sigma_-) \\ &\quad + (\lambda_1 \sin^2\theta + \lambda_2 \cos^2\theta)(b^\dagger - b)(\sigma_+ - \sigma_-) \\ &\quad - \mathrm{i}(\lambda_1 - \lambda_2)\sin\theta\cos\theta(a^\dagger + a)(\sigma_+ - \sigma_-) \\ &\quad + \mathrm{i}(\lambda_1 - \lambda_2)\sin\theta\cos\theta(b^\dagger - b)(\sigma_+ + \sigma_-). \end{aligned} \tag{52}$$

If $\lambda_1 \neq \lambda_2$, there is nothing we can know from the above equation. However, in the case of $\lambda_1 = \lambda_2 = \lambda$ ($g_1 = g_2$), we find that

$$H_U = U_\theta H U_\theta^\dagger = H_\lambda. \tag{53}$$

Therefore, the Hamiltonian H_λ is invariant under the continuous $U(1)$ transformation.

Moreover, when $g > g_c = 1$, the system enters into the EMSP in which the ground state is infinitely degenerate since for a given ground-state energy, an infinite number of values of the parameter μ in the eigenstate can be taken, as long as the condition $\alpha^2 + \beta^2 = (\eta/4)(g^2 - g^{-2})$ is satisfied. This signifies that the continuous $U(1)$ symmetry breaks down in the EMSP.

4. The excitation spectra, photon number and fluctuations of field quadratures

4.1. Excitation spectra

Since we don't know whether $|1,0\rangle$ or $|0,1\rangle$ is the first excited state, the excitation energy is the smaller one of two values of energy from $|0,0\rangle$ to $|1,0\rangle$ and $|0,1\rangle$. In the NP, when the system excites from the ground state to $|1,0\rangle$, the energy needed is the single-photon energy of cavity field a, which is given by the first expression in Eq. (6). When the system excites from the ground state to $|0,1\rangle$, the energy needed is the single-photon energy of cavity modes b, which is given by the second expression Eq. (6). The excitation energy of the whole system is

$$\varepsilon_{\rm np} = \min(\varepsilon_{1,\rm np}, \varepsilon_{2,\rm np}) = \begin{cases} \omega\sqrt{1 - g_1^2}, & g_1 \geqslant g_2, \\ \omega\sqrt{1 - g_2^2}, & g_1 < g_2. \end{cases} \tag{54}$$

In the ESP, when the system excites from the ground state to $|1,0\rangle$ and $|0,1\rangle$, two values of energy needed are respectively given by the two expressions in Eq. (18). The excitation energy of the whole system is

$$\varepsilon_{\rm esp} = \min(\varepsilon_{1,\rm esp}, \varepsilon_{2,\rm esp}) = \begin{cases} \omega\sqrt{1 - g_1^{-4}}, & g_1 g_2 \leqslant 1, \\ \omega\sqrt{1 - \frac{g_2^2}{g_1^2}}, & g_1 g_2 > 1. \end{cases} \tag{55}$$

In the MSP, when the system excites from the ground state to $|1,0\rangle$ and $|0,1\rangle$, two values of energy needed are respectively given by the two expressions in Eq. (26). The excitation energy of the whole system is

$$\varepsilon_{\rm msp} = \min(\varepsilon_{1,\rm msp}, \varepsilon_{2,\rm msp}) = \begin{cases} \omega\sqrt{1 - g_2^{-4}}, & g_1 g_2 \leqslant 1, \\ \omega\sqrt{1 - \frac{g_1^2}{g_2^2}}, & g_1 g_2 > 1. \end{cases} \tag{56}$$

In the EMSP, when the system excites from the ground state to $|1,0\rangle$ and $|0,1\rangle$, two values of energy needed are respectively given by the two expressions in Eq. (36). The excitation energy of the whole system is

$$\varepsilon_{\rm emsp} = \min(\varepsilon_{1,\rm emsp}, \varepsilon_{2,\rm emsp}) = \begin{cases} \omega\sqrt{\frac{1 - g^{-4}}{1 + \mu^2}}, & |\mu| \geqslant 1, \\ \omega\sqrt{\frac{\mu^2(1 - g^{-4})}{1 + \mu^2}}, & |\mu| < 1. \end{cases} \tag{57}$$

Therefore, we know that from the NP to the ESP, $\varepsilon \sim |g_1 - g_c|^{1/2}$, which gives its critical exponent as $1/2$. From the NP to the MSP, $\varepsilon \sim |g_2 - g_c|^{1/2}$, thus the critical exponent of excitation energy is also $1/2$. In Fig. 3, the excitation energy is shown when the system excites from the ground-state to the lowest excited state. For simplicity, we take $\omega = 1.0$. It has been shown that the breaking of continuous symmetry leads to a gapless excitation spectrum (Nambu–Goldstone mode).[68–70] There are three critical lines in this figure: $g_1 = 1, 0 \leqslant g_2 \leqslant 1$; $g_2 = 1, 0 \leqslant g_1 \leqslant 1$ and $g_1 = g_2 \geqslant g_c = 1$. The excitation energy in these three lines becomes zero. For the diagonal critical line, the continuous $U(1)$ symmetry breaks down, and the corresponding mode is the Nambu–Goldstone mode. For the system with single-mode photon, the emergence of Nambu–Goldstone needs the rotating-wave approximation and strong collective atom-photon coupling.[65,71–73] However, the rotating-wave approximation breaks down when the collective atom–photon coupling is strong. Here no rotating-wave approximation is applied and we show that Nambu–Goldstone mode can exist when the system has a strong atom–photon coupling. This phenomenon also emerges in the two-mode Dicke model.[66]

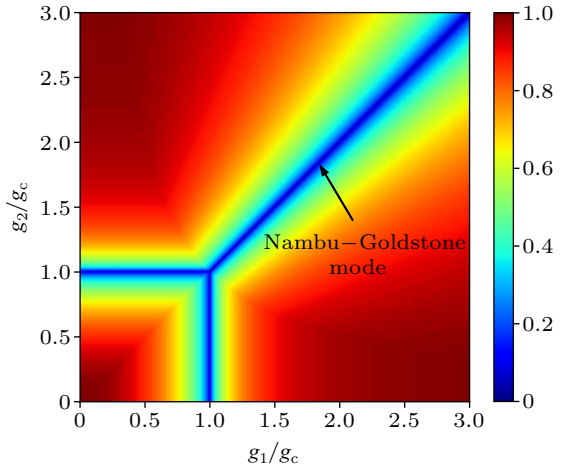


Fig. 3. The excitation spectra as a function of g_1 and g_2 with $\omega = 1.0$. There are three critical lines in this figure: $g_1 = 1, 0 \leqslant g_2 \leqslant 1$; $g_2 = 1, 0 \leqslant g_1 \leqslant 1$ and $g_1 = g_2 \geqslant g_c = 1$. The excitation energy in these three lines becomes zero. For the diagonal critical line, the continuous $U(1)$ symmetry breaks down, and the corresponding mode is the Nambu–Goldstone mode.

4.2. Critical photon number

For the NP, the rescaled average photon number of the first cavity field a in the ground state is

$$\begin{aligned} n_{1,\mathrm{np}} &= \frac{1}{\eta}\left\langle \phi^{00}_{\mathrm{np}}(g_1,g_2)\right| a^\dagger a \left|\phi^{00}_{\mathrm{np}}(g_1,g_2)\right\rangle \\ &= \frac{1}{4\eta}[(1-g_1^2)^{1/2}+(1-g_1^2)^{-1/2}-2]. \end{aligned} \tag{58}$$

Similarly, the rescaled average photon number of the second cavity field b in the ground state is

$$\begin{aligned} n_{2,\mathrm{np}} &= \frac{1}{\eta}\left\langle \phi^{00}_{\mathrm{np}}(g_1,g_2)\right| b^\dagger b \left|\phi^{00}_{\mathrm{np}}(g_1,g_2)\right\rangle \\ &= \frac{1}{4\eta}[(1-g_2^2)^{1/2}+(1-g_2^2)^{-1/2}-2]. \end{aligned} \tag{59}$$

When $\eta \to \infty$, $n_{1,\mathrm{np}} = 0$, and $n_{2,\mathrm{np}} = 0$. Therefore, there is no collective excitation for both cavity fields a and b when the system is in the NP.

For the ESP, the rescaled average photon number of the first cavity field a in the ground state is

$$\begin{aligned} n_{1,\mathrm{esp}} &= \frac{1}{\eta}{}_{\pm}\left\langle \phi^{00}_{\mathrm{esp}}(g_1,g_2)\right| a^\dagger a \left|\phi^{00}_{\mathrm{esp}}(g_1,g_2)\right\rangle_{\pm} \\ &= \frac{1}{4}(g_1^2-g_1^{-2}) \\ &\quad +\frac{1}{4\eta}\left[(1-g_1^{-4})^{1/2}+(1-g_1^{-4})^{-1/2}-2\right]. \end{aligned} \tag{60}$$

Similarly, the rescaled average photon number of the second cavity field b in the ground state is

$$\begin{aligned} n_{2,\mathrm{esp}} &= \frac{1}{\eta}{}_{\pm}\left\langle \phi^{00}_{\mathrm{esp}}(g_1,g_2)\right| b^\dagger b \left|\phi^{00}_{\mathrm{esp}}(g_1,g_2)\right\rangle_{\pm} \\ &= \frac{1}{4\eta}\left[\left(1-\frac{g_2^2}{g_1^2}\right)^{1/2}+\left(1-\frac{g_2^2}{g_1^2}\right)^{-1/2}-2\right]. \end{aligned} \tag{61}$$

When $\eta \to \infty$, $n_{1,\mathrm{esp}} = (1/4)(g_1^2 - g_1^{-2})$ and $n_{2,\mathrm{esp}} = 0$. Therefore, there is collective excitation for cavity field a but no collective excitation emerges for cavity field b. The coupling of cavity field a with atom represents the interaction of electric field and spin, that is why this phase is called the electric superradiant phase. From the NP to the ESP, the rescaled average photon number n_1 is an order parameter with critical exponent as 1.

For the MSP, the rescaled average photon number of the first cavity field a in the ground state is

$$\begin{aligned} n_{1,\mathrm{msp}} &= \frac{1}{\eta}{}_{\pm}\left\langle \phi^{00}_{\mathrm{msp}}(g_1,g_2)\right| a^\dagger a \left|\phi^{00}_{\mathrm{msp}}(g_1,g_2)\right\rangle_{\pm} \\ &= \frac{1}{4\eta}\left[\left(1-\frac{g_1^2}{g_2^2}\right)^{1/2}+\left(1-\frac{g_1^2}{g_2^2}\right)^{-1/2}-2\right]. \end{aligned} \tag{62}$$

The rescaled average photon number of the second cavity field b in the ground state is

$$\begin{aligned} n_{2,\mathrm{msp}} &= \frac{1}{\eta}{}_{\pm}\left\langle \phi^{00}_{\mathrm{msp}}(g_1,g_2)\right| b^\dagger b \left|\phi^{00}_{\mathrm{msp}}(g_1,g_2)\right\rangle_{\pm} \\ &= \frac{1}{4}(g_2^2-g_2^{-2}) \\ &\quad +\frac{1}{4\eta}\left[(1-g_2^{-4})^{1/2}+(1-g_2^{-4})^{-1/2}-2\right]. \end{aligned} \tag{63}$$

When $\eta \to \infty$, $n_{1,\mathrm{msp}} = 0$ and $n_{2,\mathrm{msp}} = (1/4)(g_2^2 - g_2^{-2})$. Therefore, there is no collective excitation for cavity field a but collective excitation emerges for cavity field b. The coupling of cavity field b with atom represents the interaction of magnetic field and spin, that is why this phase is called the magnetic superradiant phase. From the NP to the MSP, the rescaled average photon number n_2 is an order parameter with critical exponent as 1.

For the EMSP, the rescaled average photon number of the first cavity field a in the ground state is

$$\begin{aligned} n_{1,\mathrm{emsp}} &= \frac{1}{\eta}{}_{\pm}\left\langle \phi^{00}_{\mathrm{emsp}}(g)\right| a^\dagger a \left|\phi^{00}_{\mathrm{emsp}}(g)\right\rangle_{\pm} \\ &= \frac{1}{4\eta}\left[\left(\frac{1-g^{-4}}{1+\mu^2}\right)^{1/2}+\left(\frac{1-g^{-4}}{1+\mu^2}\right)^{-1/2}-2\right] \\ &\quad +\frac{1}{4(1+\mu^2)}(g^2-g^{-2}). \end{aligned} \tag{64}$$

The rescaled average photon number of the second cavity field b in the ground state is

$$\begin{aligned} n_{2,\mathrm{emsp}} &= \frac{1}{\eta}{}_{\pm}\left\langle \phi^{00}_{\mathrm{emsp}}(g)\right| b^\dagger b \left|\phi^{00}_{\mathrm{emsp}}(g)\right\rangle_{\pm} \\ &= \frac{1}{4\eta}\left[|\mu|\left(\frac{1-g^{-4}}{1+\mu^2}\right)^{1/2}+\frac{1}{|\mu|}\left(\frac{1-g^{-4}}{1+\mu^2}\right)^{-1/2}-2\right] \\ &\quad +\frac{\mu^2}{4(1+\mu^2)}(g^2-g^{-2}). \end{aligned} \tag{65}$$

When $\eta \to \infty$, $n_{1,\mathrm{emsp}} = (1/(4(1+\mu^2)))(g^2-g^{-2})$, $n_{2,\mathrm{emsp}} = (\mu^2/(4(1+\mu^2)))(g^2-g^{-2})$. Therefore, collective excitations emerge for both cavity fields a and b and this phase is called the electromagnetic superradiant phase.

4.3. The fluctuations of field quadratures

In the ground state of NP, for the first cavity field, it is not hard to obtain that the fluctuation of position operator of the first oscillator $x_1 = (a^\dagger + a)/\sqrt{2}$ is

$$\Delta x_{1,\mathrm{np}} = \sqrt{\langle x_1^2\rangle - \langle x_1\rangle^2} = \frac{1}{\sqrt{2}}(1-g_1^2)^{-1/4}. \tag{66}$$

Similarly, for the momentum operator $p_1 = \mathrm{i}(a^\dagger - a)/\sqrt{2}$, we have

$$\Delta p_{1,\mathrm{np}} = \sqrt{\langle p_1^2\rangle - \langle p_1\rangle^2} = \frac{1}{\sqrt{2}}(1-g_1^2)^{1/4}. \tag{67}$$

For the second cavity field,

$$\Delta x_{2,\mathrm{np}} = \frac{1}{\sqrt{2}}(1-g_2^2)^{1/4},\ \ \Delta p_{2,\mathrm{np}} = \frac{1}{\sqrt{2}}(1-g_2^2)^{-1/4}. \tag{68}$$

While the Δx plays an analogous role of the diverging length scale in the extended quantum system, the critical point accompanies an infinite amount of squeezing in the momentum quadrature p, so that it remains in the minimum uncertainty state for any g_1 and g_2, i.e., $\Delta x_{1,\mathrm{np}}\Delta p_{1,\mathrm{np}} = 1/2$, $\Delta x_{2,\mathrm{np}}\Delta p_{2,\mathrm{np}} = 1/2$.

In the ESP, it is not hard to obtain that the fluctuation of quadratures of the cavity field a is respectively

$$\Delta x_{1,\mathrm{esp}} = \frac{1}{\sqrt{2}}(1-g_1^{-4})^{-1/4},\ \ \Delta p_{1,\mathrm{esp}} = \frac{1}{\sqrt{2}}(1-g_1^{-4})^{1/4}. \tag{69}$$

For the cavity field b, it is easy to obtain

$$\Delta x_{2,\mathrm{esp}} = \frac{1}{\sqrt{2}}\left(1-\frac{g_2^2}{g_1^2}\right)^{1/4},\ \ \Delta p_{2,\mathrm{esp}} = \frac{1}{\sqrt{2}}\left(1-\frac{g_2^2}{g_1^2}\right)^{-1/4}. \tag{70}$$

In the MSP, the fluctuations of quadratures of the cavity field a are respectively

$$\Delta x_{1,\mathrm{msp}} = \frac{1}{\sqrt{2}}\left(1-\frac{g_1^2}{g_2^2}\right)^{-1/4},\ \ \Delta p_{1,\mathrm{msp}} = \frac{1}{\sqrt{2}}\left(1-\frac{g_1^2}{g_2^2}\right)^{1/4}. \tag{71}$$

For the second cavity field, it is easy to obtain

$$\Delta x_{2,\mathrm{msp}} = \frac{1}{\sqrt{2}}\left(1-g_2^{-4}\right)^{1/4},\ \ \Delta p_{2,\mathrm{msp}} = \frac{1}{\sqrt{2}}\left(1-g_2^{-4}\right)^{-1/4}. \tag{72}$$

In the EMSP, the fluctuations of quadratures of the cavity field a are respectively

$$\begin{cases} \Delta x_{1,\mathrm{emsp}} = \frac{1}{\sqrt{2}}\left(\frac{1-g^{-4}}{1+\mu^2}\right)^{-1/4}, \\ \Delta p_{1,\mathrm{emsp}} = \frac{1}{\sqrt{2}}\left(\frac{1-g^{-4}}{1+\mu^2}\right)^{1/4}. \end{cases} \tag{73}$$

For the cavity field b, it is easy to obtain

$$\begin{cases} \Delta x_{2,\mathrm{emsp}} = \frac{1}{\sqrt{2}}\left[\frac{\mu^2(1-g^{-4})}{1+\mu^2}\right]^{1/4}, \\ \Delta p_{2,\mathrm{emsp}} = \frac{1}{\sqrt{2}}\left[\frac{\mu^2(1-g^{-4})}{1+\mu^2}\right]^{-1/4}. \end{cases} \tag{74}$$

In the ESP, MSP and EMSP, the system also remains in the minimum uncertainty state for any g_1 and g_2, i.e., $\Delta x_1\Delta p_1 = 1/2$, $\Delta x_2\Delta p_2 = 1/2$. In the four phases, the critical exponents of Δx_1 and Δp_1 are $-1/4$ and $1/4$ respectively, which are the same with that in the single-mode QRM. However, the critical exponents of Δx_2 and Δp_2 are $1/4$ and $-1/4$ respectively, which are the opposite with that in the single-mode QRM.[15] This may be attributed to the fact that the coupling of field a with atom in our model represents the interaction of electric field with spin, which is the same as that in the single-mode QRM. However the coupling of field b with atom represents interaction of the magnetic field with spin, which is different from that in the single-mode QRM.

5. Finite-frequency scaling

To derive analytically the finite-frequency scaling exponents of important quantities, we need to take the higher-order (up to fourth order) correction of perturbation into consideration. After adding the higher-order correction, the Hamiltonian of the NP is

$$\begin{aligned} \tilde{H}_{\mathrm{np}} =\ & \omega a^\dagger a + \omega b^\dagger b + \frac{\Omega}{2}\sigma_z + \frac{\omega^2}{4\Omega}(g_1^2+g_2^2) \\ & -\frac{\omega}{4}[g_1^2(a^\dagger+a)^2 - g_2^2(b^\dagger-b)^2] \\ & +\frac{\omega^2}{2\Omega}g_1g_2(a^\dagger b + a b^\dagger) \\ & +\frac{\omega^2}{16\Omega}[g_1^2(a^\dagger+a)^2 - g_2^2(b^\dagger-b)^2]^2, \end{aligned} \tag{75}$$

where the fourth-order correction adds a quartic potential for the cavity field. The above Hamiltonian cannot be analytically diagonalized, but we can use a variational method to derive its expectation value. We propose a trial wave function of ground state as

$$\begin{aligned} |\psi_{00}(s_1,s_2)\rangle =\ & \mathcal{S}_2^\dagger(s_2)\mathcal{S}_1^\dagger(s_1)\,|0,0\rangle \\ =\ & \mathrm{e}^{-(s_2/2)(b^{\dagger 2}-b^2)}\,\mathrm{e}^{-(s_1/2)(a^{\dagger 2}-a^2)}\,|0,0\rangle, \end{aligned} \tag{76}$$

where s_1 and s_2 are variational parameters. The energy expectation value in the ground state is

$$\begin{aligned} E_{00}(s_1,s_2) =\ & \langle\psi_{00}(s_1,s_2)|\tilde{H}_{\mathrm{np}}|\psi_{00}(s_1,s_2)\rangle \\ =\ & \frac{\omega}{2}\left[\cosh(2s_1) - \frac{g_1^2}{2}\mathrm{e}^{-2s_1}\right] \\ & +\frac{\omega}{2}\left[\cosh(2s_2) - \frac{g_2^2}{2}\mathrm{e}^{2s_2}\right] \\ & +\frac{\omega^2}{16\Omega}\left[3g_1^4\mathrm{e}^{-4s_1} + 2g_1^2g_2^2\mathrm{e}^{2(s_2-s_1)}\right. \end{aligned}$$

$$+3g_2^4\mathrm{e}^{4s_2}\Big]-\frac{\Omega}{2}-\omega+\frac{\omega^2}{4\Omega}(g_1^2+g_2^2). \quad (77)$$

To decide the minimum of $E_{00}(s_1,s_2)$, it is required that

$$\begin{cases}\frac{\partial E_{00}(s_1,s_2)}{\partial s_1}=0,\\ \frac{\partial E_{00}(s_1,s_2)}{\partial s_2}=0.\end{cases} \quad (78)$$

At the critical point $g_1=g_2=g_\mathrm{c}=1$, the above equations become

$$\begin{cases}\mathrm{e}^{6s_1}-\frac{1}{2\eta}\left[\mathrm{e}^{2(s_1+s_2)}+3\right]=0,\\ \frac{1}{2\eta}\left[3\mathrm{e}^{6s_2}+\mathrm{e}^{2(2s_2-s_1)}\right]-1=0.\end{cases} \quad (79)$$

By canceling the e^{s_2} term in these equations and defining $u=\eta\,\mathrm{e}^{6s_1}$, we have

$$(u-2)(6u^2-14u+9)=0. \quad (80)$$

The three solutions for Eq. (80) are $u=2$, $(7\pm\sqrt{5}\mathrm{i})/6$. To ensure the squeezing operator $\mathcal{S}_1(s_1)$ is unitary, the parameter s_1 has to be real. Hence we have only one sensible solution $u=2$ and

$$s_1=-\frac{1}{6}\ln\frac{\eta}{2},\ \ s_2=\frac{1}{6}\ln\frac{\eta}{2}. \quad (81)$$

To know whether the extreme values we obtained are minimum, we calculate the second-order partial derivatives of $E_{00}(s_1,s_2)$ as

$$\begin{aligned}\frac{\partial^2 E_{00}}{\partial s_1^2}&=\omega\left[\mathrm{e}^{2s_1}+(1-g_1^2)\mathrm{e}^{-2s_1}\right]\\&\quad+\frac{\omega^2}{2\Omega}\left[6g_1^4\mathrm{e}^{-4s_1}+g_1^2g_2^2\mathrm{e}^{2(s_2-s_1)}\right], \quad (82)\\ \frac{\partial^2 E_{00}}{\partial s_2^2}&=\omega\left[(1-g_2^2)\mathrm{e}^{2s_2}+\mathrm{e}^{-2s_2}\right]\\&\quad+\frac{\omega^2}{2\Omega}\left[6g_2^4\mathrm{e}^{4s_2}+g_1^2g_2^2\mathrm{e}^{2(s_2-s_1)}\right]. \quad (83)\end{aligned}$$

It is evident that $\partial^2E_{00}/\partial s_1^2>0$ and $\partial^2E_{00}/\partial s_2^2>0$. Therefore, we have the minimum point as the critical parameters

$$\begin{aligned}(s_{1\mathrm{c}},s_{2\mathrm{c}})&=[s_1(\eta,g_1,g_2),s_2(\eta,g_1,g_2)]_{\min}|_{g_1=g_2=g_\mathrm{c}}\\&=\left(-\frac{1}{6}\ln\frac{\eta}{2},\frac{1}{6}\ln\frac{\eta}{2}\right). \quad (84)\end{aligned}$$

Substituting the above values of s_1 and s_2 into Eq. (77), we can obtain the minimum expectation value of energy corresponding to the trial wave function as the approximation of ground-state energy

$$E_{00}(s_{1\mathrm{c}},s_{2\mathrm{c}})=\frac{3\omega}{4}\left(\frac{\eta}{2}\right)^{-1/3}+\frac{\omega}{4}\left(\frac{\eta}{2}\right)^{-1}-\frac{\Omega}{2}-\omega. \quad (85)$$

When the higher-order correction is not taken into consideration, the ground-state energy in the NP at the critical point is $E_{\mathrm{G,np}}(g_1=g_2=g_\mathrm{c})=-(\Omega/2)-\omega$. Thus we can obtain the finite-frequency correction for the rescaled ground-state energy at critical point is

$$\begin{aligned}&e_\mathrm{G}(\eta,g_1=g_2=g_\mathrm{c})\\&=\frac{1}{\eta}\left[E_{00}(s_{1\mathrm{c}},s_{2\mathrm{c}})-E_{\mathrm{G,np}}(g_1=g_2=g_\mathrm{c})\right]\\&=\frac{3\omega}{8}\left(\frac{\eta}{2}\right)^{-\frac{4}{3}}+\frac{\omega}{8}\left(\frac{\eta}{2}\right)^{-2}. \quad (86)\end{aligned}$$

The rescaled cavity photon number of cavity field a is

$$\begin{aligned}&n_{1\mathrm{c}}(\eta,g_1=g_2=g_\mathrm{c})\\&=\frac{1}{\eta}\langle\psi_{00}(s_{1\mathrm{c}},s_{2\mathrm{c}})|a^\dagger a|\psi_{00}(s_{1\mathrm{c}},s_{2\mathrm{c}})\rangle\\&=\frac{1}{8}\left(\frac{\eta}{2}\right)^{-2/3}-\frac{1}{4}\left(\frac{\eta}{2}\right)^{-1}+\frac{1}{8}\left(\frac{\eta}{2}\right)^{-4/3}. \quad (87)\end{aligned}$$

The rescaled cavity photon number of cavity field b is

$$\begin{aligned}&n_{2\mathrm{c}}(\eta,g_1=g_2=g_\mathrm{c})\\&=\frac{1}{\eta}\langle\psi_{00}(s_{1\mathrm{c}},s_{2\mathrm{c}})|b^\dagger b|\psi_{00}(s_{1\mathrm{c}},s_{2\mathrm{c}})\rangle\\&=\frac{1}{8}\left(\frac{\eta}{2}\right)^{-2/3}-\frac{1}{4}\left(\frac{\eta}{2}\right)^{-1}+\frac{1}{8}\left(\frac{\eta}{2}\right)^{-4/3}. \quad (88)\end{aligned}$$

The finite-frequency scaling exponents of e_G, $n_{1\mathrm{c}}$ and $n_{2\mathrm{c}}$ are found to be same as those of corresponding observables for the one-mode QRM,[15] Dicke model[74] and LMG model.[75,76] The leading-order corrections of the fluctuations of cavity field quadratures of mode a are respectively

$$\begin{cases}\Delta x_1(\eta,g_1=g_2=g_\mathrm{c})=\frac{1}{\sqrt{2}}\left(\frac{\eta}{2}\right)^{1/6},\\ \Delta p_1(\eta,g_1=g_2=g_\mathrm{c})=\frac{1}{\sqrt{2}}\left(\frac{\eta}{2}\right)^{-1/6}.\end{cases} \quad (89)$$

The leading-order corrections of the fluctuations of cavity field quadratures of mode b are respectively

$$\begin{cases}\Delta x_2(\eta,g_1=g_2=g_\mathrm{c})=\frac{1}{\sqrt{2}}\left(\frac{\eta}{2}\right)^{-1/6},\\ \Delta p_2(\eta,g_1=g_2=g_\mathrm{c})=\frac{1}{\sqrt{2}}\left(\frac{\eta}{2}\right)^{1/6}.\end{cases} \quad (90)$$

We assume that the excited states corresponding to the quantum number m_1,m_2 are

$$\mathcal{S}_2^\dagger[s_{2,\min}(\eta,g_1,g_2)]\mathcal{S}_1^\dagger[s_{1,\min}(\eta,g_1,g_2)]\,|m_1,m_2\rangle,$$

where $(s_{1,\min},s_{2,\min})$ is a pair of parameters for the ground-state energy to achieve its minimum. The energy gap between the states $\mathcal{S}_2^\dagger[s_{2,\min}(\eta,g_1,g_2)]\mathcal{S}_1^\dagger[s_{1,\min}(\eta,g_1,g_2)]\,|n_1,n_2\rangle$ and $\mathcal{S}_2^\dagger[s_{2,\min}(\eta,g_1,g_2)]\mathcal{S}_1^\dagger[s_{1,\min}(\eta,g_1,g_2)]\,|m_1,m_2\rangle$ at the quadruple point is

$$\begin{aligned}\varepsilon(\eta,g=g_\mathrm{c})&=\langle m_1,m_2|\mathcal{S}_2\mathcal{S}_1H_\mathrm{np}\mathcal{S}_1^\dagger\mathcal{S}_2^\dagger|m_1,m_2\rangle\\&\quad-\langle n_1,n_2|\mathcal{S}_2\mathcal{S}_1H_\mathrm{np}\mathcal{S}_1^\dagger\mathcal{S}_2^\dagger|n_1,n_2\rangle. \quad (91)\end{aligned}$$

At the critical point, substituting the relevant parameters and simplifying the result, we can obtain

$$\varepsilon(\eta,g=g_\mathrm{c})=\frac{\omega}{16}\left(\frac{\eta}{2}\right)^{-1/3}\Big[3(m_1^2+m_2^2-n_1^2-n_2^2)$$

$$+13(m_1+m_2-n_1-n_2)$$
$$+4(m_1m_2-n_1n_2)\Big]. \tag{92}$$

For the cavity field a, the energy correction from the ground state ($n_1=0,n_2=0$) to the first excitation state ($m_1=1,m_2=0$) is

$$\varepsilon_{1,g_c}(\eta)=\omega\left(\frac{\eta}{2}\right)^{-1/3}. \tag{93}$$

For the cavity field b, the energy correction from the ground state ($n_1=0,n_2=0$) to the first excitation state ($m_1=0,m_2=1$) is

$$\varepsilon_{2,g_c}(\eta)=\omega\left(\frac{\eta}{2}\right)^{-1/3}, \tag{94}$$

which is the same with that of cavity field a. Therefore, for the whole system, the correction of excitation energy is

$$\varepsilon_{g_c}(\eta)=\omega\left(\frac{\eta}{2}\right)^{-1/3}. \tag{95}$$

Now we confirm the validity of the low-energy effective Hamiltonians in Eqs. (4), (15), (23), and (33). For the phase transition from the NP to the ESP, according to the scaling theory of phase transition, the critical behavior of the average photon number of cavity field a at critical point is $n_1\sim|g_1-g_c|^{\gamma}\sim\eta^{-\gamma/\nu}$, $(g_1\to g_c)$, where γ and ν are the critical exponents of n_1 and η respectively. The finite-frequency scaling ansatz predicts that, for a large η and near the critical point, the expectation value of n_1 can be written in terms of a variable-dependent scaling function $f_1(x)$

$$n_1\eta^{\gamma/\nu}=f_1[(g_1-g_c)\eta^{1/\nu}]. \tag{96}$$

From Subsection 4.2 and Eq. (87), we know that $\gamma=1$, and the finite-frequency scaling exponent of n_1 is $-\gamma/\nu=-2/3$. Therefore, we have $\nu=3/2$. Equation (96) becomes

$$n_1\eta^{2/3}=f_1[(g_1-g_c)\eta^{2/3}]. \tag{97}$$

If all the data about n_1 calculated from numerically diagonalizing the two-mode quantum Rabi Hamiltonian Eq. (1) for many various g_1 and η is plotted in a rescaled axis, there must be a single curve that reveals the scaling function $f_1(x)$. In Fig. 4, one can indeed see that all curves collapse into a single curve, revealing an observable-dependent scaling function $f_1(x)$.

For the phase transition from the NP to the MSP, there is a similar scaling relation for the averaged photon number n_2

$$n_2\eta^{2/3}=f_2[(g_2-g_c)\eta^{2/3}], \tag{98}$$

where $f_2(x)$ is another scaling function. The expectation values n_2 for various g_2 and η are plotted in Fig. 5, from which one can see that all curves collapse into a single curve. Based on the numerical confirmation, we conclude that the effective Hamiltonians in Eqs. (4), (15), (23), and (33) are indeed correct low-energy effective Hamiltonians of the two-mode QRM in the limit $\eta\to\infty$.

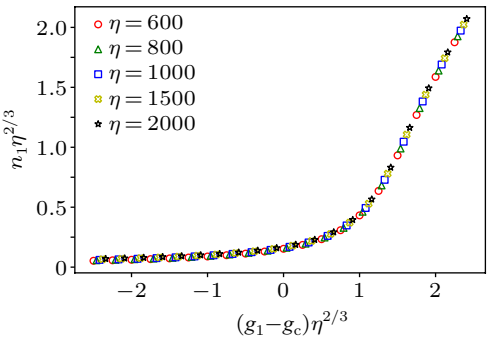


Fig. 4. For the phase transition from NP to ESP, the values of averaged photon number n_1 calculated by numerically diagonalizing the two-mode quantum Rabi Hamiltonian for many various g_1 and η are plotted in a rescaled axis. One can clearly see that all curves collapse into a single curve, revealing an observable-dependent scaling function $f_1(x)$.

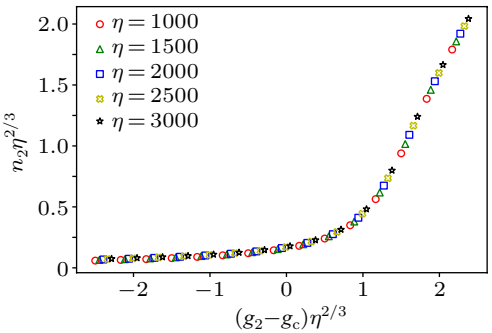


Fig. 5. For the phase transition from NP to MSP, the values of averaged photon number n_2 calculated by numerically diagonalizing the two-mode quantum Rabi Hamiltonian for many various g_2 and η are plotted in a rescaled axis. One can clearly see that all curves collapse into a single curve, revealing an observable-dependent scaling function $f_2(x)$.

6. Summary and conclusions

We investigate the ground-state phase diagram, symmetries, excitation spectra and finite-frequency scaling of the two-mode quantum Rabi model. Based on the Schrieffer–Wolff transformation, we obtain the low-energy effective Hamiltonians for various phases of two-mode quantum Rabi model, by which we find the quartic critical point and a rich phase diagram, including a normal phase, an electric superradiant phase, a magnetic superradiant phase and an electromagnetic superradiant phase. The phase transitions from the normal phase to the electric (magnetic) superradiant phase are of second order with the averaged photon number as order parameter, and associate with the breaking of a discrete Z_2 symmetry, while the phase transition from the electric superradiant phase to the magnetic superradiant phase is of first order. If the collective atom–photon coupling strength parameters are equal, there is a continuous $U(1)$ symmetry, which breaks down in the electromagnetic superradiant phase because the ground state of this phase is infinitely degenerate. We calculate analytically the excitation energy, photon number and fluctuations of field quadratures. In the excitation spectra, there are

three critical lines in which the excitation energy becomes zero and the Nambu–Goldstone mode is found. The critical exponents of excitation energy and photon number are the same with those of the single-mode quantum Rabi model. The critical exponents of Δx and Δp of the first cavity field a in the four phases are the same with those in the single-mode quantum Rabi model, while the critical exponents of the Δx and Δp of the second cavity field b are the opposite with that in the single-mode quantum Rabi model. At last, in order to confirm the validity of the low-energy effective Hamiltonians of four phases analytically derived by us, we obtain the analytical finite-frequency scaling exponents and verify the finite-frequency scaling relation of averaged photon number of two cavity fields by numerically diagonalizing the two-mode quantum Rabi Hamiltonian. The results show that all data for many different g_1 (g_2) and η collapses into a single curve, concluding that the Hamiltonians we calculated are correct in the limit $\eta \to \infty$.

Appendix A: Derivation of effective Hamiltonian

In this section, we give detailed derivation of low-energy effective Hamiltonians and ground-state energy by the Schrieffer–Wolff (SW) transformation. Based on the idea of perturbation theory, H can be written in the form of

$$H = H_0 + V, \tag{A1}$$

where

$$H_0 = \omega a^\dagger a + \omega b^\dagger b + \frac{\Omega}{2}\sigma_z, \tag{A2}$$

$$\begin{aligned} V &= \lambda_1(a^\dagger + a)(\sigma_+ + \sigma_-) + \lambda_2(b^\dagger - b)(\sigma_+ - \sigma_-) \\ &= \sqrt{2}(\lambda_1 x_1 \sigma_x + \lambda_2 p_2 \sigma_y), \end{aligned} \tag{A3}$$

where $x_1 = (a^\dagger + a)/\sqrt{2}$ and $p_2 = \mathrm{i}(b^\dagger - b)/\sqrt{2}$. The eigenvalues and eigenvectors of H_0 are given by

$$E^{(0)}_{\pm,m_1,m_2} = (m_1+m_2)\omega \pm \frac{\Omega}{2}, \quad |\uparrow(\downarrow), m_1, m_2\rangle. \tag{A4}$$

According to Schrieffer–Wolff (SW) transformation, we need to find a unitary operator $U = \mathrm{e}^S$ such that the transformation $\tilde{H} = UHU^\dagger$ converts H into a block-diagonal form. Define a superoperator L as

$$LA = [S, A]. \tag{A5}$$

We expand S and L in series

$$S = \sum_{n=1}^{\infty} S_n, \quad L = \sum_{n=1}^{\infty} L_n, \tag{A6}$$

where $L_n A = [S_n, A]$. If we split V into block-diagonal part V_d and block-off-diagonal V_od, the leading-order terms of S are

$$S_1 = L_0^{-1} V_\mathrm{od}, \tag{A7}$$

$$S_2 = L_0^{-1} L_1 V_\mathrm{d}, \tag{A8}$$

$$S_3 = -\frac{1}{3} L_0^{-1} L_1^3 H_0 + L_0^{-1} L_2 V_\mathrm{d}, \tag{A9}$$

where $L_0 A = [H_0, A]$ and

$$L_0^{-1} A = -\mathrm{i} \lim_{\kappa \to 0} \int_0^\infty \mathrm{e}^{-\kappa t}\, \mathrm{e}^{\mathrm{i}H_0 t} A\, \mathrm{e}^{-\mathrm{i}H_0 t}\, \mathrm{d}t \tag{A10}$$

for an arbitrary operator A. The leading-order terms of low-energy effective Hamiltonian (up to fourth order) are given by

$$\tilde{H}^{(1)} = P V_\mathrm{d} P, \tag{A11}$$

$$\tilde{H}^{(2)} = (1/2) P L_1 V_\mathrm{od} P, \tag{A12}$$

$$\tilde{H}^{(3)} = (1/2) P L_2 V_\mathrm{od} P, \tag{A13}$$

$$\tilde{H}^{(4)} = (1/2) P L_3 V_\mathrm{od} P - \frac{1}{24} P L_1^3 V_\mathrm{od} P, \tag{A14}$$

where $P = |\downarrow\rangle\langle\downarrow|$ is the project operator onto the low-energy space.

For the Hamiltonian of two-mode QRM, it is not hard to confirm that the perturbation Eq. (A3) is block-off-diagonal, namely, $V_\mathrm{d} = 0$ and $V_\mathrm{od} = V$. Therefore, we have $S_2 = 0$ and $\tilde{H}^{(1)} = \tilde{H}^{(3)} = 0$.

Now we calculate S_1. According to Eqs. (A7) and (A10),

$$S_1 = -\mathrm{i} \lim_{\kappa \to 0} \int_0^\infty \mathrm{e}^{-\kappa t}\, \mathrm{e}^{\mathrm{i}H_0 t} V_\mathrm{od}\, \mathrm{e}^{-\mathrm{i}H_0 t}\, \mathrm{d}t. \tag{A15}$$

We need to first calculate the temporal evolution of V_od,

$$\begin{aligned} V_\mathrm{od}(t) &= \mathrm{e}^{\mathrm{i}H_0 t} V_\mathrm{od}\, \mathrm{e}^{-\mathrm{i}H_0 t} \\ &= \sqrt{2}\lambda_1\, \mathrm{e}^{\mathrm{i}\omega a^\dagger a t} x_1\, \mathrm{e}^{-\mathrm{i}\omega a^\dagger a t}\, \mathrm{e}^{\mathrm{i}\frac{\Omega}{2}\sigma_z t} \sigma_x\, \mathrm{e}^{-\mathrm{i}\frac{\Omega}{2}\sigma_z t} \\ &\quad + \sqrt{2}\lambda_2\, \mathrm{e}^{\mathrm{i}\omega b^\dagger b t} p_2\, \mathrm{e}^{-\mathrm{i}\omega b^\dagger b t}\, \mathrm{e}^{\mathrm{i}\frac{\Omega}{2}\sigma_z t} \sigma_y\, \mathrm{e}^{-\mathrm{i}\frac{\Omega}{2}\sigma_z t}. \end{aligned} \tag{A16}$$

For a one-dimensional harmonic oscillator with Hamiltonian $\omega a^\dagger a$, the temporal evolution of position x and momentum p can be derived by the Heisenberg equation as

$$\begin{cases} x(t) = \mathrm{e}^{\mathrm{i}\omega a^\dagger a t} x \mathrm{e}^{-\mathrm{i}\omega a^\dagger a t} = x\cos(\omega t) + p\sin(\omega t), \\ p(t) = \mathrm{e}^{\mathrm{i}\omega a^\dagger a t} p \mathrm{e}^{-\mathrm{i}\omega a^\dagger a t} = p\cos(\omega t) - x\sin(\omega t), \end{cases} \tag{A17}$$

where $x = x(0)$ and $p = p(0)$.

Substituting Eq. (A17) into Eq. (A16) and using operator relation $\mathrm{e}^{\mathrm{i}\sigma_z\theta} = \cos\theta + \mathrm{i}\sigma_z \sin\theta$, then substituting the result into Eq. (A15), we obtain

$$\begin{aligned} S_1 &= \frac{\sqrt{2}\mathrm{i}}{\Omega^2 - \omega^2}\Big[\lambda_1(\Omega x_1 \sigma_y + \omega p_1 \sigma_x) \\ &\quad - \lambda_2(\omega x_2 \sigma_y + \Omega p_2 \sigma_x)\Big] \\ &= \frac{\sqrt{2}\mathrm{i}\Omega}{\Omega^2 - \omega^2}(\lambda_1 x_1 \sigma_y - \lambda_2 p_2 \sigma_x) + \mathcal{O}\left(\frac{\lambda_{1,2}\omega}{\Omega^2}\right) \\ &= \frac{\Omega}{\Omega^2 - \omega^2}[\lambda_1(a^\dagger + a)(\sigma_+ - \sigma_-) \\ &\quad + \lambda_2(b^\dagger - b)(\sigma_+ + \sigma_-)] + \mathcal{O}\left(\frac{\lambda_{1,2}\omega}{\Omega^2}\right). \end{aligned} \tag{A18}$$

In order to evaluate S_3, we need to calculate $L_1^3 H_0 = [S_1,[S_1,[S_1,H_0]]]$. From Eq. (A7) we know that

$$[S_1,H_0] = -V. \tag{A19}$$

After neglecting the high-order small quantities, we can obtain

$$\begin{aligned}[S_1,[S_1,H_0]] &= -[S_1,V] \\ &\approx -\frac{2\Omega}{\Omega^2-\omega^2}[\lambda_1^2(a^\dagger+a)^2\sigma_z \\ &\quad -\lambda_2^2(b^\dagger-b)^2\sigma_z], \end{aligned} \tag{A20}$$

$$\begin{aligned} L_1^3 H_0 &= [S_1,[S_1,[S_1,H_0]]] \\ &\approx \frac{8\sqrt{2}\Omega^2}{(\Omega^2-\omega^2)^2}(\lambda_1^3 x_1^3\sigma_x + \lambda_1^2\lambda_2 x_1^2 p_2\sigma_y \\ &\quad +\lambda_1\lambda_2^2 x_1 p_2^2\sigma_x + \lambda_2^3 p_2^3\sigma_y). \end{aligned} \tag{A21}$$

Since $V_\mathrm{d}=0$, the second term in the right side of Eq. (A9) vanishes. Similar to the procedure of calculating S_1, we can obtain

$$\begin{aligned} S_3 &= -\frac{4\Omega^5}{3(\Omega^2-\omega^2)^3(\Omega^2-9\omega^2)}\Big[\lambda_1^3(a^\dagger+a)^3(\sigma_+-\sigma_-) \\ &\quad +\lambda_1^2\lambda_2(a^\dagger+a)^2(b^\dagger-b)(\sigma_++\sigma_-) \\ &\quad -\lambda_1\lambda_2^2(a^\dagger+a)(b^\dagger-b)^2(\sigma_+-\sigma_-) \\ &\quad -\lambda_2^3(b^\dagger-b)^3(\sigma_++\sigma_-)\Big] + \mathcal{O}\left(\frac{\lambda_{1,2}^3\omega}{\Omega^4}\right). \end{aligned} \tag{A22}$$

According to Eqs. (A12) and (A14), $\tilde{H}^{(2)}$ and $\tilde{H}^{(4)}$ can be calculated as

$$\tilde{H}^{(2)} \approx -\frac{\Omega}{\Omega^2-\omega^2}[\lambda_1^2(a^\dagger+a)^2 - \lambda_2^2(b^\dagger-b)^2], \tag{A23}$$

$$\tilde{H}^{(4)} \approx \frac{\Omega^3(\Omega^2+3\omega^2)}{(\Omega^2-\omega^2)^3(\Omega^2-9\omega^2)}[\lambda_1^2(a^\dagger+a)^2 - \lambda_2^2(b^\dagger-b)^2]^2. \tag{A24}$$

Summing up the above results, the low-energy effective Hamiltonian is

$$\begin{aligned} H_\mathrm{eff} &\approx \omega a^\dagger a + \omega b^\dagger b + \frac{\Omega}{2}\sigma_z \\ &\quad -\frac{\Omega}{\Omega^2-\omega^2}[\lambda_1^2(a^\dagger+a)^2 - \lambda_2^2(b^\dagger-b)^2] \\ &\quad +\frac{\Omega^3(\Omega^2+3\omega^3)}{(\Omega^2-\omega^2)^3(\Omega^2-9\omega^2)}\Big[\lambda_1^2(a^\dagger+a)^2 \\ &\quad -\lambda_2^2(b^\dagger-b)^2\Big]^2. \end{aligned} \tag{A25}$$

Under the condition $\Omega \gg \omega$, $\tilde{H}^{(2)}$ and $\tilde{H}^{(4)}$ can be simplified, thus we have

$$\begin{aligned} H_\mathrm{eff} &\approx \omega a^\dagger a + \omega b^\dagger b + \frac{\Omega}{2}\sigma_z \\ &\quad -\frac{1}{\Omega}\left[\lambda_1^2(a^\dagger+a)^2 - \lambda_2^2(b^\dagger-b)^2\right] \\ &\quad +\frac{1}{\Omega^3}\left[\lambda_1^2(a^\dagger+a)^2 - \lambda_2^2(b^\dagger-b)^2\right]^2. \end{aligned} \tag{A26}$$

Considering the limit $\eta = \Omega/\omega \to \infty$, and projecting the Hamiltonian to the spin-down subspace, we can obtain the effective Hamiltonian of the normal phase (NP) as

$$H_\mathrm{np} = \omega a^\dagger a + \omega b^\dagger b - \frac{\Omega}{2} - \frac{1}{\Omega}[\lambda_1^2(a^\dagger+a)^2 - \lambda_2^2(b^\dagger-b)^2]. \tag{A27}$$

By applying unitary transformations with squeezing operators $\mathcal{S}_1(r_{1,\mathrm{np}}) = \exp[(r_{1,\mathrm{np}}/2)(a^{\dagger 2}-a^2)]$ and $\mathcal{S}_2(r_{2,\mathrm{np}}) = \exp[(r_{2,\mathrm{np}}/2)(b^{\dagger 2}-b^2)]$ to H_np and using equation $\mathrm{e}^{-B}A\,\mathrm{e}^{B} = \sum_{n=0}^{\infty}[A,B]^{(n)}$, where $[A,B]^{(n)} = [[A,B]^{(n-1)},B]$ with $[A,B]^{(0)} = A$, we can obtain

$$\begin{aligned} H'_\mathrm{np} &= \omega\left[\cosh(2r_{1,\mathrm{np}}) - \frac{g_1^2}{2}\mathrm{e}^{-2r_{1,\mathrm{np}}}\right]a^\dagger a \\ &\quad +\omega\left[\cosh(2r_{2,\mathrm{np}}) - \frac{g_2^2}{2}\mathrm{e}^{2r_{2,\mathrm{np}}}\right]b^\dagger b \\ &\quad -\frac{\omega}{2}\left[\sinh(2r_{1,\mathrm{np}}) + \frac{g_1^2}{2}\mathrm{e}^{-2r_{1,\mathrm{np}}}\right](a^{\dagger 2}+a^2) \\ &\quad -\frac{\omega}{2}\left[\sinh(2r_{2,\mathrm{np}}) - \frac{g_2^2}{2}\mathrm{e}^{2r_{2,\mathrm{np}}}\right](b^{\dagger 2}+b^2) \\ &\quad +\frac{\omega}{2}\left[\cosh(2r_{1,\mathrm{np}}) - \frac{g_1^2}{2}\mathrm{e}^{-2r_{1,\mathrm{np}}}\right] \\ &\quad +\frac{\omega}{2}\left[\cosh(2r_{2,\mathrm{np}}) - \frac{g_2^2}{2}\mathrm{e}^{2r_{2,\mathrm{np}}}\right] - \frac{\Omega}{2} - \omega, \end{aligned} \tag{A28}$$

where $g_1 = 2\lambda_1/\sqrt{\omega\Omega}$ and $g_2 = 2\lambda_2/\sqrt{\omega\Omega}$. Since the new Hamiltonian needs to be diagonal, we require that $(a^{\dagger 2}+a^2)$ and $(b^{\dagger 2}+b^2)$ terms vanish, therefore

$$\begin{cases} \sinh(2r_{1,\mathrm{np}}) + \frac{g_1^2}{2}\mathrm{e}^{-2r_{1,\mathrm{np}}} = 0, \\ \sinh(2r_{2,\mathrm{np}}) - \frac{g_2^2}{2}\mathrm{e}^{2r_{2,\mathrm{np}}} = 0. \end{cases} \tag{A29}$$

Their solutions are

$$r_{1,\mathrm{np}} = \frac{1}{4}\ln(1-g_1^2), \quad r_{2,\mathrm{np}} = -\frac{1}{4}\ln(1-g_2^2). \tag{A30}$$

Substituting these solutions to Eq. (A28), the diagonalized Hamiltonian can be obtained as

$$H'_\mathrm{np} = \varepsilon_{1,\mathrm{np}}a^\dagger a + \varepsilon_{2,\mathrm{np}}b^\dagger b + E_{\mathrm{G,np}}, \tag{A31}$$

where

$$\varepsilon_{1,\mathrm{np}} = \omega\sqrt{1-g_1^2}, \quad \varepsilon_{2,\mathrm{np}} = \omega\sqrt{1-g_2^2} \tag{A32}$$

are the excitation energy of two cavity fields respectively and

$$E_{\mathrm{G,np}} = (1/2)(\varepsilon_{1,\mathrm{np}}+\varepsilon_{2,\mathrm{np}}) - \omega - \frac{\Omega}{2} \tag{A33}$$

is the ground-state energy. The energy eigenvalues and eigenstates in the NP are respectively

$$E_\mathrm{np}^{m_1m_2}(g_1,g_2) = \varepsilon_{1,\mathrm{np}}m_1 + \varepsilon_{2,\mathrm{np}}m_2 + E_{\mathrm{G,np}}, \tag{A34}$$

$$\left|\phi_{\rm np}^{m_1m_2}(g_1,g_2)\right\rangle = \mathcal{S}_2^{\dagger}[r_{2,\rm np}(g_2)]\mathcal{S}_1^{\dagger}[r_{1,\rm np}(g_1)]\left|m_1,m_2,\downarrow\right\rangle. \tag{A35}$$

Since $E_{\rm G,np}$ must be real, for the NP we have $g_1 \leqslant 1,\ g_2 \leqslant 1$.

For $g_1 > 1$ or $g_2 > 1$, the discussion and calculations are given in the main text.

Acknowledgments

We thank Gaoke Hu for his helpful discussion on the finite-frequency scaling. This work was supported by the National Natural Science Foundation of China (Grant No. 12135003). The authors acknowledge HPC Cluster of ITP-CAS for supplying computation resources.

References

[1] Fink J M, Dombi A, Vukics A, Wallraff A and Domokos P 2017 *Phys. Rev. X* **7** 011012
[2] Sun Z H, Cai J Q, Tang Q C, Hu Y and Fan H 2020 *Ann. Phys.* **532** 1900270
[3] Casteels W, Fazio R and Ciuti C 2017 *Phys. Rev. A* **95** 012128
[4] Zhu H J, Xu K, Zhang G F and Liu W M 2020 *Phys. Rev. Lett.* **125** 050402
[5] Garbe L, Bina M, Keller A, Paris M G A and Felicetti S 2020 *Phys. Rev. Lett.* **124** 120504
[6] Puebla R, Smirne A, Huelga S F and Plenio M B 2020 *Phys. Rev. Lett.* **124** 230602
[7] Chen X Y, Zhang Y Y, Fu L and Zheng H 2020 *Phys. Rev. A* **101** 033827
[8] Zhang Y, Mao B B, Xu D, Zhang Y Y, You W L, Liu M and Luo H G 2020 *J. Phys. A: Math. Theor.* **53** 315302
[9] Forn-Díaz P, Lamata L, Rico E, Kono J and Solano E 2019 *Rev. Mod. Phys.* **91** 025005
[10] Zhu C J, Ping L L, Yang Y P and Agarwal G S 2020 *Phys. Rev. Lett.* **124** 073602
[11] Wang Y Z, He S, Duan L and Chen Q H 2021 *Phys. Rev. B* **103** 205106
[12] Leppäkangas J, Braumüller J, Hauck M, Reiner J M, Schwenk I, Zanker S, Fritz L, Ustinov A V, Weides M and Marthaler M 2018 *Phys. Rev. A* **97** 052321
[13] Abdi M 2019 *Phys. Rev. B* **100** 184310
[14] Garbe L, Egusquiza I L, Solano E, Ciuti C, Coudreau T, Milman P and Felicetti S 2017 *Phys. Rev. A* **95** 053854
[15] Hwang M J, Puebla R and Plenio M B 2015 *Phys. Rev. Lett.* **115** 180404
[16] Xie Q, Zhong H, Batchelor M T and Lee C 2017 *J. Phys. A: Math. Theor.* **50** 113001
[17] Rabi I I 1936 *Phys. Rev.* **49** 324
[18] Rabi I I 1937 *Phys. Rev.* **51** 652
[19] Jaynes E and Cummings F 1963 *Proc. IEEE* **51** 89
[20] Raimond J M, Brune M and Haroche S 2001 *Rev. Mod. Phys.* **73** 565
[21] Holstein T 1959 *Ann. Phys.* **8** 325
[22] Crespi A, Longhi S and Osellame R 2012 *Phys. Rev. Lett.* **108** 163601
[23] Cai M L, Liu Z D, Zhao W D, Wu Y K, Mei Q X, Jiang Y, He L, Zhang X, Zhou Z C and Duan L M 2021 *Nat. Commun.* **12** 1126
[24] Chen X, Wu Z, Jiang M, Lü X Y, Peng X and Du J 2021 *Nat. Commun.* **12** 6281
[25] Blais A, Huang R S, Wallraff A, Girvin S M and Schoelkopf R J 2004 *Phys. Rev. A* **69** 062320
[26] Wallraff A, Schuster D I, Blais A, Frunzio L, Huang R S, Majer J, Kumar S, Girvin S M and Schoelkopf R J 2004 *Nature* **431** 162
[27] Niemczyk T, Deppe F, Huebl H, Menzel E P, Hocke F, Schwarz M J, Garcia-Ripoll J J, Zueco D, Hümmer T, Solano E, Marx A and Gross R 2010 *Nat. Phys.* **6** 772
[28] Forn-Díaz P, Lisenfeld J, Marcos D, García-Ripoll J J, Solano E, Harmans C J P M and Mooij J E 2010 *Phys. Rev. Lett.* **105** 237001
[29] Chen Z, Wang Y, Li T, Tian L, Qiu Y, Inomata K, Yoshihara F, Han S, Nori F, Tsai J S and You J Q 2017 *Phys. Rev. A* **96** 012325
[30] Forn-Díaz P, García-Ripoll J J, Peropadre B, Orgiazzi J L, Yurtalan M A, Belyansky R, Wilson C M and Lupascu A 2017 *Nat. Phys.* **13** 39
[31] Yoshihara F, Fuse T, Ashhab S, Kakuyanagi K, Saito S and Semba K 2017 *Nat. Phys.* **13** 44
[32] Irish E K 2007 *Phys. Rev. Lett.* **99** 173601
[33] Irish E K 2007 *Phys. Rev. Lett.* **99** 259901
[34] Zhong H, Xie Q, Batchelor M T and Lee C 2013 *J. Phys. A: Math. Theor.* **46** 415302
[35] Xie Q T, Cui S, Cao J P, Amico L and Fan H 2014 *Phys. Rev. X* **4** 021046
[36] Ying Z J, Liu M, Luo H G, Lin H Q and You J Q 2015 *Phys. Rev. A* **92** 053823
[37] Casanova J, Romero G, Lizuain I, García-Ripoll J J and Solano E 2010 *Phys. Rev. Lett.* **105** 263603
[38] Gan C J and Zheng H 2010 *Eur. Phys. J. D* **59** 473
[39] Braak D 2011 *Phys. Rev. Lett.* **107** 100401
[40] Larson J 2012 *Phys. Rev. Lett.* **108** 033601
[41] Yu L, Zhu S, Liang Q, Chen G and Jia S 2012 *Phys. Rev. A* **86** 015803
[42] Chen Q H, Wang C, He S, Liu T and Wang K L 2012 *Phys. Rev. A* **86** 023822
[43] Ashhab S 2013 *Phys. Rev. A* **87** 013826
[44] De Liberato S 2014 *Phys. Rev. Lett.* **112** 016401
[45] Liu M, Ying Z J, An J H and Luo H G 2015 *New J. Phys.* **17** 043001
[46] Cong L, Sun X M, Liu M, Ying Z J and Luo H G 2017 *Phys. Rev. A* **95** 063803
[47] Wang Y, You W L, Liu M, Dong Y L, Luo H G, Romero G and You J Q 2018 *New J. Phys.* **20** 053061
[48] Mao B B, Li L, Wang Y, You W L, Wu W, Liu M and Luo H G 2019 *Phys. Rev. A* **99** 033834
[49] Mahmoodian S 2019 *Phys. Rev. Lett.* **123** 133603
[50] Kockum A F, Miranowicz A, De Liberato S, Savasta S and Nori F 2019 *Nat. Rev. Phys.* **1** 295
[51] Forn-Díaz P, Lamata L, Rico E, Kono J and Solano E 2019 *Rev. Mod. Phys.* **91** 025005
[52] Xie W, Mao B B, Li G, Wang W, Sun C, Wang Y, You W L and Liu M 2020 *J. Phys. A: Math. Theor.* **53** 095302
[53] Le Boité A 2020 *Adv. Quantum Technol.* **3** 1900140
[54] Frisk K A, Miranowicz A, De Liberato S, Savasta S and Nori F 2019 *Nat. Rev. Phys.* **1** 19
[55] Liu M, Chesi S, Ying Z J, Chen X, Luo H G and Lin H Q 2017 *Phys. Rev. Lett.* **119** 220601
[56] Boller K J, Imamoğlu A and Harris S E 1991 *Phys. Rev. Lett.* **66** 2593
[57] Fleischhauer M and Lukin M D 2000 *Phys. Rev. Lett.* **84** 5094
[58] Bergmann K, Theuer H and Shore B W 1998 *Rev. Mod. Phys.* **70** 1003
[59] Bruß D and Macchiavello C 2002 *Phys. Rev. Lett.* **88** 127901
[60] Cerf N J, Bourennane M, Karlsson A and Gisin N 2002 *Phys. Rev. Lett.* **88** 127902
[61] Zhou Z, Chu S I and Han S 2002 *Phys. Rev. B* **66** 054527
[62] Sjöqvist E, Tong D M, Andersson L M, Hessmo B, Johansson M and Singh K 2012 *New J. Phys.* **14** 103035
[63] Hayn M, Emary C and Brandes T 2011 *Phys. Rev. A* **84** 053856
[64] Cordero S, Nahmad-Achar E, López-Peña R and Castaños O 2015 *Phys. Rev. A* **92** 053843
[65] Baksic A and Ciuti C 2014 *Phys. Rev. Lett.* **112** 173601
[66] Fan J, Yang Z, Zhang Y, Ma J, Chen G and Jia S 2014 *Phys. Rev. A* **89** 023812
[67] Léonard J, Morales A, Zupancic P, Esslinger T and Donner T 2017 *Nature* **543** 87
[68] Nambu Y and Jona-Lasinio G 1961 *Phys. Rev.* **122** 345
[69] Goldstone J 1961 *Il Nuovo Cimento* **19** 154
[70] Goldstone J, Salam A and Weinberg S 1962 *Phys. Rev.* **127** 965
[71] Popov V N and Fedotov S A 1982 *Theor. Math. Phys.* **51** 363
[72] Ye J and Zhang C 2011 *Phys. Rev. A* **84** 023840
[73] Yu Y X, Ye J and Liu W M 2013 *Sci. Rep.* **3** 3476
[74] Vidal J and Dusuel S 2006 *Europhys. Lett.* **74** 817
[75] Dusuel S and Vidal J 2004 *Phys. Rev. Lett.* **93** 237204
[76] Dusuel S and Vidal J 2005 *Phys. Rev. B* **71** 224420